TERAHERTZ SPECTRAL IMAGING TECHNIQUES IN NDT: TOPOGRAPHY AND COMPUTED TOMOGRAPHY

Benjamin EWERS*, Andreas KUPSCH, Axel LANGE, Manfred P. HENTSCHEL

BAM FEDERAL INSTITUTE FOR MATERIALS RESEARCH AND TESTING, 12200 Berlin, Germany
*present address: PHILIPPS-UNIVERSITÄT MARBURG, 35032 Marburg, Germany

Abstract

The emerging technology of generation and detection of Terahertz waves (1 THz = 10^{12} Hz) offers diverse potentials in non-destructive testing (NDT) regarding security as well as safety aspects. Herein, we focus on the latter with emphasis on imaging techniques.
The THz range (0.1 … 10 THz, 3mm …30 µm) closes the technological gap between ultra high frequency electronics and FIR optics in the electro-magnetic (EM) spectrum. Electro-optical sampling provides straight access to the EM wave including its phase (rather than intensity). THz waves are well suited to characterize non-metallic materials since they penetrate paper, plastics, ceramics and certain composites (e.g. GFC).
We employ a commercial fibre-coupled THz time domain spectrometer (TDS) for scanning the samples laterally through a focal spot. At each position the entire temporal pulse train is recorded, which offers the opportunity to use various parameters derivable for imaging.
Topographic measurements are performed as reflection set-up. The achievable spatial resolution is diffraction limited at about 100 µm -300 µm (which allows for perception of single defects on a sub-mm scale). In contrast to typical pulse echoed ultrasound testing THz topography is a non-contact inspection tool without coupling agents. Several reflections of subsequent concealed layers are detected instead of just the first encountered one. Comparing to X-ray (radiology) the non-ionizing THz-waves generate images of similar contrast regarding metal and plastic (organic) components, while conventional radiography emphasizes one type of material depending on the energy pre-selected. Moreover, the full temporal information is exploited to derive spectra in certain selected time windows, i.e. separated spectral properties of each layer in multilayered structures.
Tomographic measurements are performed in transmission mode. The sample is mounted on a rotation stage in order to allow for lateral scanning under the different projection angles. The reconstruction is typically performed by filtered backprojection, which is widely used for X-ray CT. The adaption of this technique to the THz range comes along with several experimental drawbacks such as considerable refraction and scattering. According to these difficulties we investigate the occurring artefacts. The THz-TDS provides the opportunity to calculate a separate backprojection of each frequency interval as obtained by the Fourier transformation of the recorded time resolved amplitude. This results in a spectrally resolved reconstruction of each voxel, which is unique in computed tomography technology.
Keywords: Terahertz Time Domain Spectroscopy, Spectral Computed Tomography, 3D Topography

1 Introduction

Terahertz (THz) radiation has enforced public attention since body scanners have been installed at some European airports in recent years. From a technical point of view they provide excellent images revealing (illicit) items concealed beneath the clothes of persons. However, from ethical aspects their application is rather questionable, since the body's shape is made visible, as well.
Besides security applications there are promising applications in non-destructive testing (NDT) of materials. This refers for instance to the characterization of coatings, homogeneity, pores and cracks in plastics and ceramics as well as glass fibre composites. One of the most popular THz applications had been the detection of flaws (voids and disbonds) within the sprayed on foam insulation of the space shuttle external tank [1].
The term 'THz band' refers to the spectral range between 100 GHz and 10 THz of electro-magnetic waves. It closes the gap between technically mature applications of the adjacent ranges: high-frequency electronics in the GHz band (millimeter waves) used for radar, broadcasting and communication and techniques in the infrared optical range on the high-frequency side.
The (logarithmic) mean frequency of 1 THz (=10^{12} Hz) equals a wavelength of 300 μm, a wavenumber of 33.3 cm^{-1} or a photon energy of 4.1 meV. This corresponds to the energy range of thermal excitations and implies the drawback that established infrared laser technologies, which are based on creating a population inversion, cannot be transferred straightforwardly to the low energy THz range at ambient temperatures. Thus, the term 'THz gap' had been frequently used due the difficult technical access.
The technological progress during the last two decades opened up the way for practical THz applications in science and technology. Besides the electro-optical generation and detection, which is described in detail below, different cw (continuous wave) sources such as lasers and black body radiators are used. Cw radiation is commonly detected by bolometric or pyrometric sensors. Pulsed THz waves are detected by coherent techniques which offers the advantage to measure the incident electric field (incl. its sign) instead of the bare intensity.
The potential of the THz range is its superiority to other parts of the spectrum regarding certain aspects: the better spatial resolution and broad-band spectral information compared to millimeter waves, the transparency of clothes and packaging material, which are opaque at optical frequencies, and its inherent harmlessness to biological tissue (such as the human body) compared to X-rays. A disadvantage of THz practical applications is the considerable absorption in humid atmosphere due to the polarity of water molecules.

2 Interaction with matter

THz waves sample the material's dielectric properties. Macroscopically, the electric field, E, is measured after passing the matter. Inside the material, the electric field causes polarization effects, which are expressed by the physical value P. In classical electromagnetism the superposition of both fields in matter is given by the electric displacement field $D=\varepsilon_0 E+P$, where $\varepsilon_0=8.85\cdot10^{-12}$ F/m indicates the vacuum permittivity. By displacing bound electric charges the incident electric field generates dipoles p, which are excited to forced oscillations.

In case the incident wave's frequency is far from eigenfrequencies the fields E and P oscillate with the same phase ($P<\varepsilon_0 E$). In the vicinity of resonant frequencies, which correspond to molecular rotational modes in the THz range, there is a phase difference between driving (E) and forced oscillation (P). Analogously to mechanical oscillations, this implies the existence of a damping term. Usually, the relation of D and E is given by the relative permittivity ε_r: $D=\varepsilon_0\varepsilon_r E$. The phase shift mentioned above can only be realized by a complex-valued ε_r. Thus, the refractive index n_r, being the square root of ε_r, must be complex as well: $n_r=\varepsilon_r^{1/2}=n-i\kappa$.
A plane wave of angular frequency $\omega=2\pi f$ propagating in z-direction in vacuum can be expressed as $E(z,t)=E_0\exp[i\omega(t-z/c_0)]$ (c_0 being the speed of light in vacuum). Due to conservation of energy the time dependent term is neglected in the following. After penetrating matter of the thickness d the electric field is denoted as $E(z=d)=E_0\exp[-i\omega n_r d/c_0]= E_0\exp[-\omega\kappa d/c_0]\exp[i\omega n d/c_0]$. Obviously, the first exponential term describes the amplitude's attenuation (damping), whereas the second term describes the wave's phase. The phase difference of vacuum and material wave are correlated with the optical path.
According to the Maxwell's law the continuity of the electric and magnetic field components leads to the (complex) reflection and transmission coefficients, which are multiplied by the exponential terms.

3 Terahertz Time Domain Spectroscopy

3.1 Measurement principle and setup

In the following we refer to electro-optical generation and detection, exclusively. A photography of our laboratory setup is displayed in Fig. 1.
The technique of generation and detection of the THz spectrum is based on the electro-optical principle of the Auston switch [2]. Terahertz Time Domain Spectroscopy (THz TDS) is a coherent emission and detection technique with the potential to sample picosecond pulses on a femtosecond time scale. Both, emission and detection are based on the same principle. A femtosecond laser pulse generates electron-hole pairs in an electrically biased semiconductor. The laser energy corresponds to the bandgap of the semiconductor. The lifetime of the electron-hole pairs is rather short. The highly mobile carriers are accelerated towards the electrodes: for a short time the electric charges flow. After the pulse impact the current decreases rapidly due to the recombination of the electron hole pairs. According to Maxwell's laws the temporal derivative of current is proportional to the (far) electric field. In case of the short laser pulse impact the changing current generates an electric-magnetic wave in the THz range. The detection works analogous, however, the receiver antenna is not biased. The electric charges are rather accelerated by the incident THz wave instead of the bias, thus inducing a current. This current is pre-amplified and digitized by an AD converter.

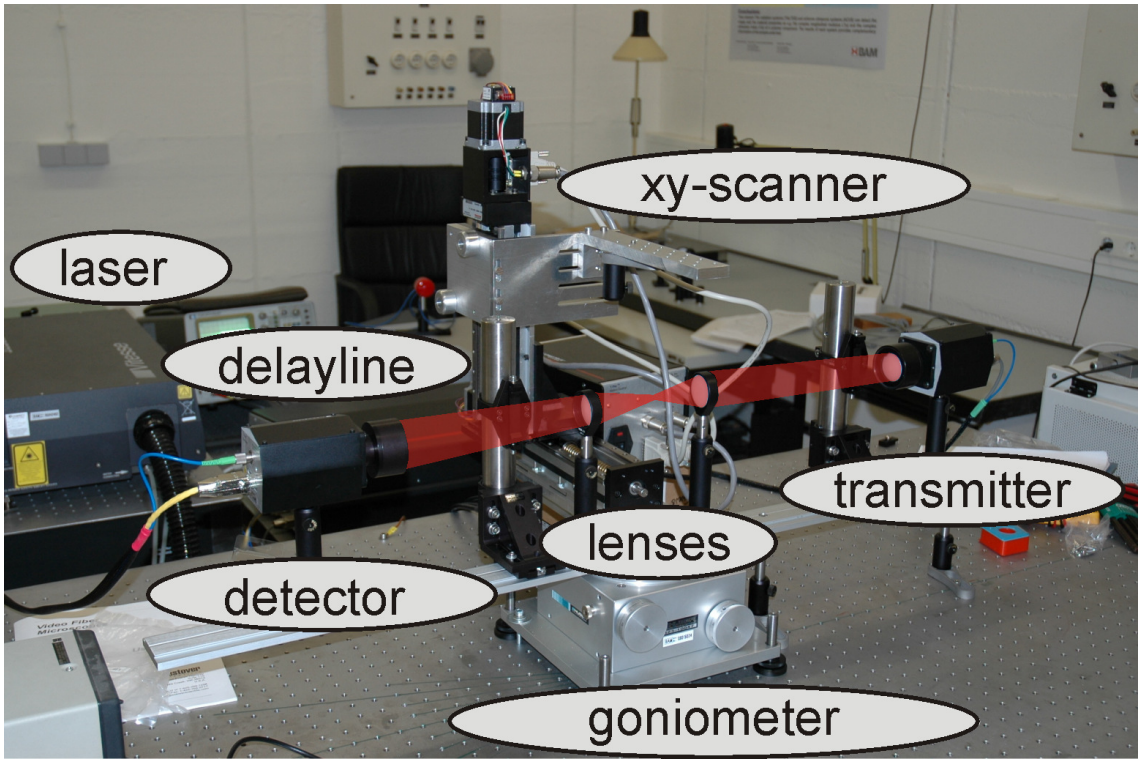

Fig. 1: Laboratory view of the THz TDS and designation of components..

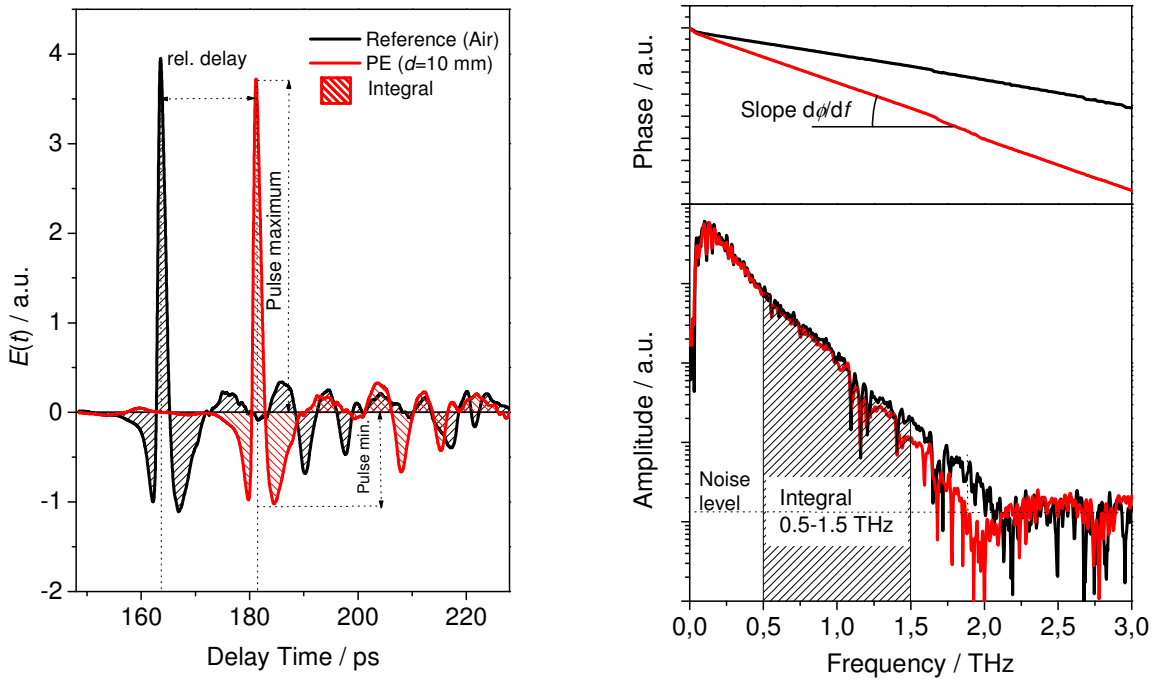

Fig. 2: Measured raw data of a polyethylene sample and reference (air) in the time domain (left), and the respective magnitude and phase of frequency components as obtained by Fourier transformation (right). The indicated quantities are a selection of scalars, which can be utilized for imaging .

The delayline provides an incremental variation of the temporal distance of laser pulses hitting the emitter and receiver antenna, thus enabling the time-resolved detection. By means of Fourier transformation the spectral information is obtained from the as-measured electric field.
The delayline can be operated in two modes: a slow scan in order to obtain highly resolved spectral data and a so-called rapid scan for imaging, where a corner cube mirror oscillates with a frequency of 20 Hz.

3.2 Imaging

Results of standard imaging in transmission setup of test specimens of well defined geometry (polyethylene step wedge), spectral imaging of explosives and IEDs (explosive devices) have been reported elsewhere [3]. Comparison has been drawn to standard NDT techniques such as ultrasonic and eddy current measurements as well as X-ray radiography and X-ray back scattering. All these results refer to imaging of a selected scalar quantity. Images can be classified into three categories: according to their origin in the time domain or the Fourier space (i.e. frequency or energy, resp.), and images of physical quantities (e.g. refractive index or absorption at selected frequencies). The respective value is directly converted to grey values or pseudocolors. Since the entire temporal pulse is measured at each position, the numerous scalars available can be combined as real spectral images. Some quantities, which can be utilized for imaging are indicated in Fig. 2.
Herein, we focus on advanced imaging techniques, which are suited tools to extract and localize features in 3-dimensional space. The standard transmission setup is used for tomographic measurements (Fig. 3, left): under each angle of rotation the specimen is scanned in the horizontal direction. The normal incidence reflection setup (Fig. 3, right) is applied for topographic (spectral *and* time-of-flight) measurements.

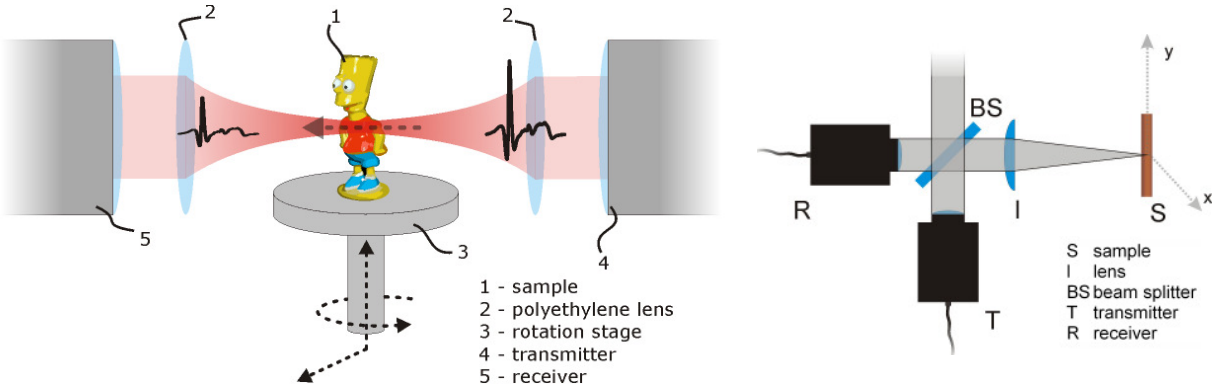

Fig. 3: THz TDS measurement setups: transmission mode (incl. rotation stage as used for tomography, left) and normal incidence reflection setup (as used for topography, right).

4 THz Spectral Computed Tomography

The first THz based computed tomography was demonstrated by Ferguson *et al.* [4]. The sample is scanned laterally in two directions under different angles of rotation (around its body axis, see Fig. 3). The whole transmitted waveform in the incident

direction is recorded at every position to obtain a spectral resolved 2D image at every angle of rotation.
One of our first measured samples was a small plastic figure (15×18×40 mm3). It was scanned with a horizontal step width of 0.5 mm, a vertical step width of 1 mm, and an angular increment of 3.6 degrees. At every step the whole time resolved waveform of the transmitted THz pulse was recorded and the spectrum was calculated by fast Fourier transformation (FFT).

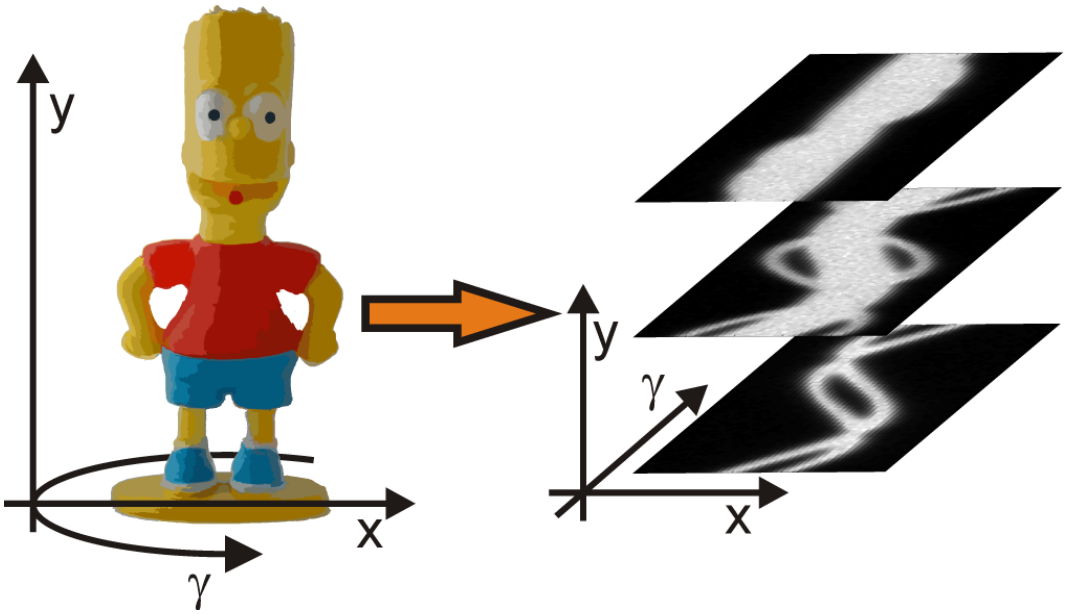

Fig. 4: Illustration of sample manipulation and the resulting data at the example of transmitted intensity at 0.8 THz. The resulting data are illustrated in so-called sinograms.

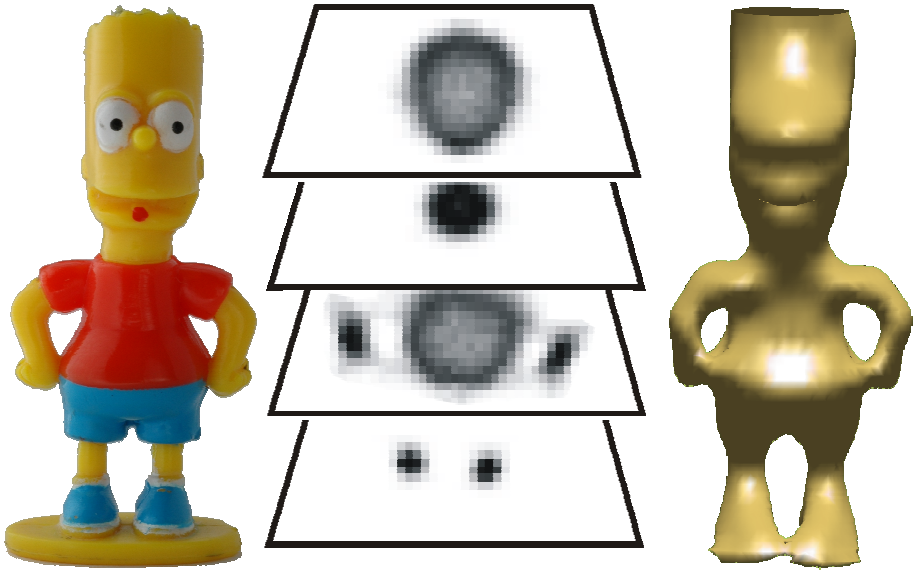

Fig. 5: Illustration of the reconstruction of a small plastic figure. From left to right: a photograph of the plastic figure (15×18×40mm3), the reconstructed averaged absorbance at four significant slices, and the visualization of the outer surface of the figure.

The recorded data can be depicted in so-called sinograms [5]. Each line of a sinogram represents a single 1D projection under a certain rotation angle γ. Stacking those lines according to γ yields a 2D intensity modulated map. An additional degree of freedom in the perpendicular linear axis results in a number of sinograms (Fig. 4).
A reconstruction of the averaged absorbance is illustrated in Fig. 5. It displays a photograph of the small plastic figure, four slices of the reconstructed absorbance, and a 3D reconstruction calculated from all reconstructed slices and visualized with the help of an isosurface algorithm.
Regions near the surface of the sample exhibit an increased absorbance as to be seen from the individual slices, which is due to the Fresnel losses that occur at the surfaces preferentially.
This significant increase is not based on the actual absorption characteristics of the material that is examined. It is rather an artefact that occurs due to the optical characteristics of the THz radiation. These characteristics are not considered in such simple reconstruction algorithm as filtered backprojection (FBP). One advantage of the time-domain-spectroscopy technique is the acquisition of a wide spectral range with a repetition rate of more than 10 Hz. This offers a spectrally resolved computed tomography. To obtain the spectral absorbance of each voxel we computed a separate reconstruction for each frequency we achieve by the prior FFT calculations. The absorbance of an arbitrary voxel is then described by the superimposition of all reconstructions. In Fig. 6 the frequency resolved absorbance is plotted at three different positions of a characteristic slice of the small plastic figure. For all frequencies the apparent absorbance of the surface region is significantly increased with respect to the inner region.

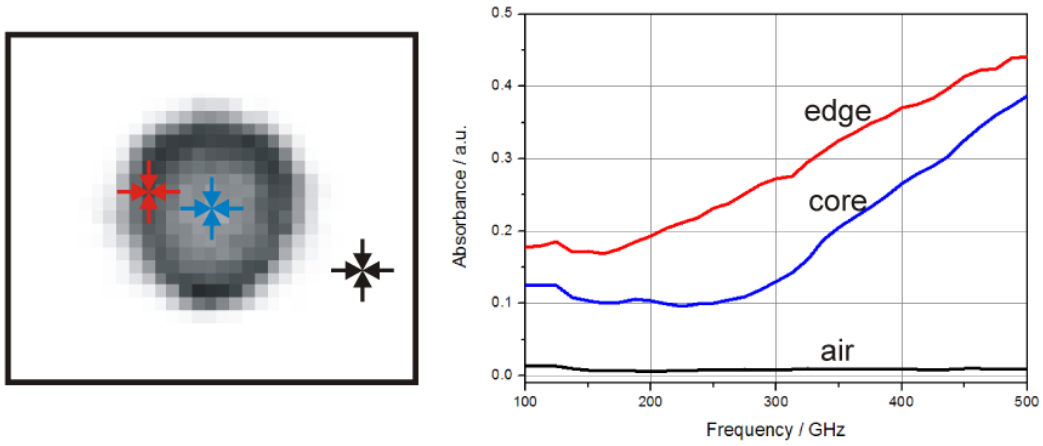

Fig. 6: Left: Averaged reconstructed absorbance (head of the figure). Right: Frequency resolved reconstructed absorbance at three different regions. The line colour corresponds to the coloured sites in the left frame.

5 THz 3D Topography

In 1997 Mittleman *et al.* [6] first demonstrated how to use the time-of-flight (TOF) signature, i.e. delayed pulse portions in the as-measured time domain to generate a T-Ray topograph of a 3.5” floppy disc.
Choosing examples of everyday communication electronics we demonstrate the perceptibility of micro- and mesostructures. We employ a normal incidence reflection setup (Fig. 3, right). The incident and reflected waves are separated by means of a beam

splitter (a silicon waver under 45 degrees). A lateral array of 70×120 mm^2 is scanned with 0.25 mm step width in order to cover a mobile music player's full size. At each position the electric field is sampled at 4096 positions in a 80 ps window resulting in a theoretical spectral resolution of 12.5 GHz. The same experimental data set is used to compute a 3D isosurface (Fig. 8) and the spectrally resolved layers (Fig. 9).

The as-measured time domain is inspected for significant peaks, i.e. delayed pulses, at each site, and the detected peak positions are merged into one histogram for all sites afterwards (Fig. 7). Pile-ups in the histogram indicate reflecting layers at distinguished depths (incl. a small variance). Retrieving those positions in the individual time domains and matching to the respective lateral position leads to connected surface areas in 3D space.

This results in a 3D-isosurface image (Fig. 8) of buried structural elements such as jog dials, resistors, ICs, display layers, plastic clippings, and cables. Moreover, the full temporal information can be exploited.

Analogous to the principle of short time Fourier transformation (STFT) we derive spectra from equidistant time windows, i.e. spectral properties of pre-selected depths. (However, these depths are chosen arbitrarily so far, regardless of the actual temporal position of layers detected.) The derived spectra are evaluated by means of relative weights of the spectral components and recorded in the color planes of a RGB image at each depth interval (Fig. 9).

Currently, our effort is on creating a recursive algorithm for evaluating the changes of the respective incident spectrum by adjacent layers.

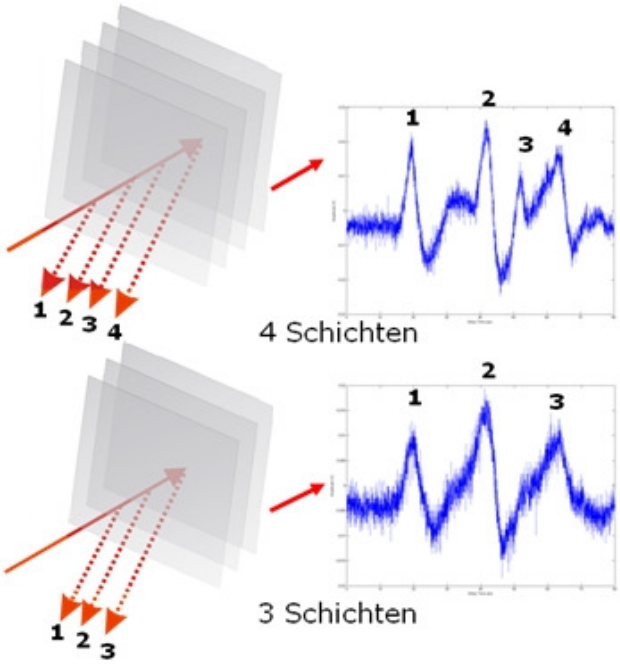

Fig. 7: Schematic drawing of THz pulses reflected from a multilayer system. The partially transparent layers reflect a portion of the incident pulse. Single reflecting layers are identified by means of delayed pulse portions due to the high (temporal) sampling rate of the applied spectrometer.

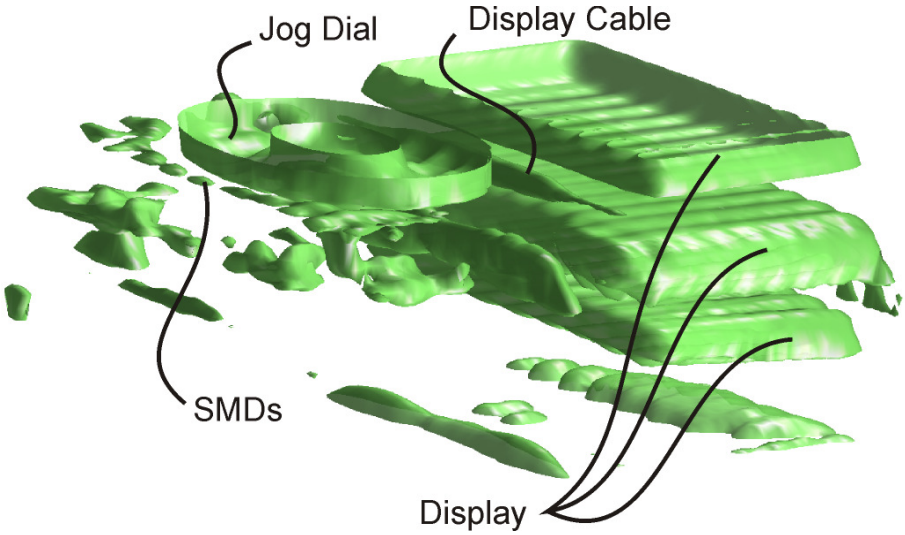

Fig. 8: Isosurface image of a mobile music player revealing the jog dial and the layered display as large components. The vertical axis carries the optical depth information as extracted by the TOF signature.

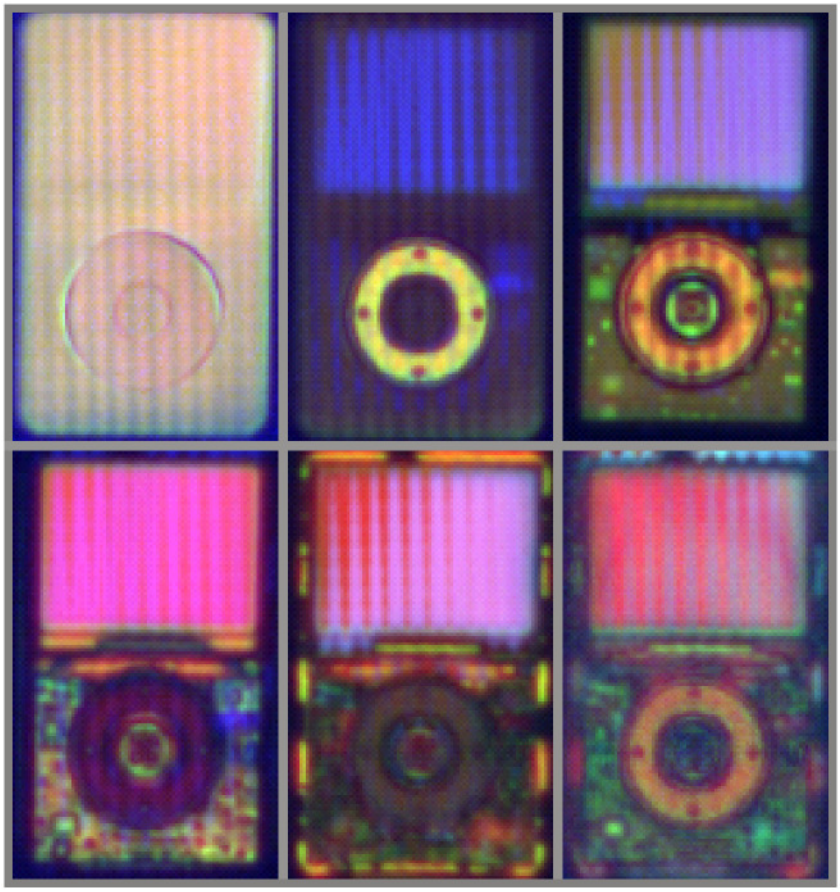

Fig. 9: Different layers of a mobile music player. The fundamental colours (red, green, blue) correspond to three different intervals in frequency domain, i.e. the normalised sum over all amplitudes of the first frequency interval is equal to the amplitude of the red color channel, etc. (increasing depth: left to right, top to bottom). Different structures such as ICs, plastic clippings, and cables are separated by colour and depth.

References

[1] D. Zimdars, J.S. White, G. Stuk, A. Chernovski, G. Fichter, S. Williamson: Large area terahertz imaging and non-destructive evaluation applications. Insight **48** (2006) 537-539.

[2] D.H. Auston, K.P. Cheung, P.R. Smith: Picosecond photoconducting Hertzian dipoles. Appl. Phys. Lett. **45** (1984) 284-286.

[3] A.Kupsch, J. Beckmann, U. Ewert, M.P. Hentschel, A. Lange: Terahertz-Wellen: Radiographie ohne Strahlengefährdung. MP Materials Testing **50** (6) (2008) 341-348.

[4] B. Ferguson, S.H. Wang, D. Gray, D. Abbot, X.C. Zhang: T-ray computed tomography. Opt. Lett. **27**, (2002) 1312-1314.

[5] A.C. Kak; M. Slaney: Principles of computerized tomographic imaging. Classics in Applied Mathematics **33**, siam (2001) and IEEE Press, New York (1988).

[6] D.M. Mittleman, S. Hunsche, L. Boivin, M.C. Nuss: T-ray tomography. Appl. Phys. B. **68** (1997), 1085-1094.